

## The Crop Generator: Implementing crop rotations to effectively advance eco-hydrological modelling

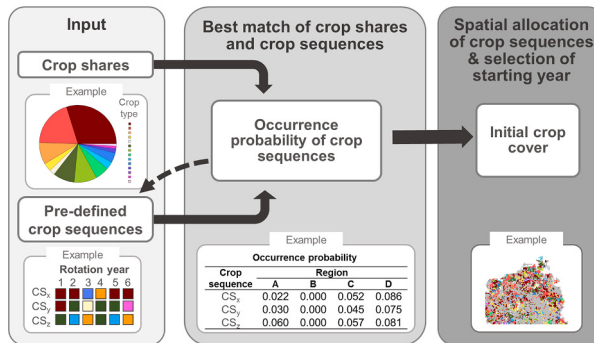
Diana Sietz <sup>\*</sup>, Tobias Conradt, Valentina Krysanova, Fred F. Hattermann, Frank Wechsung

Potsdam Institute for Climate Impact Research (PIK), Member of the Leibniz Association, P.O. Box 60 12 03, D-14412 Potsdam, Germany

### HIGHLIGHTS

- Eco-hydrological models mainly neglect crop rotations due to a lack of well-resolved multi-year crop cover data.
- We designed the Crop Generator to reproduce crop rotations at regional scale emphasising their stochastic characteristics.
- Emulating farmers' crop rotation decisions, the Crop Generator reproduces regional cropping patterns well.
- Implementation of crop rotations influences outputs of an eco-hydrological model, as illustrated by higher daily discharge.
- Crop Generator enables more realistic projections for the future and scenario impact analysis.

### GRAPHICAL ABSTRACT



### ARTICLE INFO

Editor: Dr Mark van Wijk

**Keywords:**  
Agro-ecosystem  
Land use pattern  
Quadratic programming  
Hydrological sensitivity  
Macroscale  
Sustainable agriculture

### ABSTRACT

**CONTEXT:** Crop rotations considerably affect the hydrological regime of river basins used for agricultural production and are key for sustainable land and water management. However, eco-hydrological modelling usually neglects crop rotations.

**OBJECTIVE:** In this paper, we present a Crop Generator to reproduce the stochastic characteristics of crop rotations at regional scale.

**METHODS:** The Crop Generator emulates farmers' decision making on crop rotation planning. We combined the Crop Generator with the eco-hydrological Soil and Water Integrated Model to show the hydrological relevance of considering crop rotations in a study region in central Europe including the Elbe River basin.

**RESULTS AND CONCLUSIONS:** A spatial validation showed that the Crop Generator reproduced the given cropping patterns well. Higher daily discharge, runoff and groundwater seepage and lower evapotranspiration were simulated based on crop rotations compared with a simplified representation of cropping patterns. The Crop Generator is a solution to simulate more realistic cropping patterns in large-scale eco-hydrological modelling. It closes the gap between aggregated agricultural statistics and the requirement of representing crop rotations in a realistic way in eco-hydrological modelling.

\* Corresponding author.

E-mail addresses: [sietz@pik-potsdam.de](mailto:sietz@pik-potsdam.de) (D. Sietz), [conradt@pik-potsdam.de](mailto:conradt@pik-potsdam.de) (T. Conradt), [krysanova@pik-potsdam.de](mailto:krysanova@pik-potsdam.de) (V. Krysanova), [hattermann@pik-potsdam.de](mailto:hattermann@pik-potsdam.de) (F.F. Hattermann), [Frank.Wechsung@pik-potsdam.de](mailto:Frank.Wechsung@pik-potsdam.de) (F. Wechsung).

**SIGNIFICANCE:** The Crop Generator enables smart projections of future adjustments in crop rotations in view of climate and socio-economic changes as a basis for improving eco-hydrological projections and designing more sustainable agricultural systems.

## 1. Introduction

Crop rotation is one of the oldest and most fundamental practices used in agriculture (Lawes and Gilbert, 1894; Sedlmayr, 1927). Crop rotations are planned schemes that farmers use to change crops within and between years at field level (Koennecke, 1967; Martin et al., 1976). These schemes serve to preserve soil fertility, break pest life cycles, provide a mix of food, fodder and cash crops and control insects, pathogens and undesirable plants. Replacement of formerly diverse crop rotations with monocultural cropping systems has often caused environmental problems such as a depletion of water resources (Dalin et al., 2017), soil erosion (Montgomery, 2007) and biodiversity loss (Dudley and Alexander, 2017). Hence crop rotations are essential elements in sustainable agricultural management (Bainard et al., 2017; Barbieri et al., 2017; Franke et al., 2018; Grahmann et al., 2020). Despite their relevance, eco-hydrological models largely neglect current rotation schemes limiting our capability to quantify the effects of agricultural decision making at landscape scale.

Eco-hydrological models have been used to explore how land use including agriculture affects the water balance at river basin scales (Krysanova et al., 1998; Srinivasan et al., 2010; Peng et al., 2015; Pérez-Gutiérrez and Kumar, 2019). Lack of empirical, multi-year crop data at high spatial resolution (Rounsevell et al., 2003; Srinivasan et al., 2010; Schönhart et al., 2011) severely constrains the implementation of crop rotations in eco-hydrological modelling. Recent eco-hydrological model applications considered only a few crops (mostly 2–5) arranged in short sequences (Srinivasan et al., 2010; Epelde et al., 2015; Gao et al., 2017; Bauwe et al., 2019). These were re-constructed from available, yet insufficiently resolved crop cover data or, in exceptional cases, from detailed local field maps obtained from farmers. The simplification and spatial restriction indicate fundamental sources of uncertainty and inconsistency with regional agricultural statistics, implying potential over- or underestimation of hydrological impacts of agricultural land use.

To reduce the gap to reality in these models, farmers' decision making on the design of crop rotations can be emulated. This implies a description and formalisation of the logic that farmers apply in arranging crops in space and time. Economic models used to develop or optimise locally suited crop rotations at farm and landscape scales capture the underlying decisions related to agronomic criteria, local environmental conditions, economic considerations and agricultural policies (Maxime et al., 1995; Rounsevell et al., 2003; Dogliotti et al., 2004; Schönhart et al., 2011; Dury et al., 2012). These economic models mainly apply linear programming and evolutionary optimisation algorithms to mechanistically determine optimal rotational schemes subject to a set of resource constraints and considerations of profitability, predictability and suitability (Dury et al., 2012). In these approaches, defining the model constraints and objectives is inherently difficult and the interpretation of results is often challenging. Adding to these difficulties, the representation of crop rotations at the regional scale entails great complexity due to the pronounced diversity of individual farmers' decisions.

As a way forward, this paper aims to reproduce crop rotations at regional scale with a special emphasis on their stochastic characteristics. To achieve this aim, we assume a given portfolio of crops that farmers need to combine in space and time focussing only on the final step of the crop rotation decision making. We present the Crop Generator that emulates the individual decision making at the regional scale and combine it with the eco-hydrological Soil and Water Integrated Model (SWIM). This serves to simulate inter-annual land use dynamics and

explore the sensitivity of hydrological simulations to crop rotations compared with a simplified representation of cropping patterns.

## 2. Materials and methods

### 2.1. Case study region

We developed and applied the Crop Generator to test the hydrological sensitivity of SWIM to crop rotations in a case study region in central Europe which covers eastern Germany, Czech Republic and Slovakia and includes the Elbe River basin (Fig. 1). The model domain covers the extent of a pre-defined case study area of the EU-funded research project SIM4NEXUS (2017–2020) for which SWIM had been set up. It was adopted for this study because the region comprises a climatic gradient and a broad spectrum of agricultural landscapes in central Europe. Although oriented towards historical political boundaries (German Democratic Republic, Czechoslovakia), the model domain includes the entire Elbe River basin (148,268 km<sup>2</sup>) to allow proper river runoff modelling.

The region is representative of a central European region where water shortages during summer limit plant growth and crop yields. The long-term mean annual precipitation in the entire Elbe basin is 628 mm (<500 mm in some central agricultural lowland parts) and the long-term mean discharge at the estuary is 861 m<sup>3</sup>.s<sup>-1</sup> (Simon et al., 2005) equalling 183 mm per year and 29% of precipitation. According to the 2012 version of the CORINE land cover map (CLC, 2012), 40% of the model domain (40% of Elbe River basin) are »non-irrigated arable land«. This is the most frequent land use class followed by 19% (22% of Elbe River basin) of coniferous forests concentrated in mountainous areas. Forests in general (including broad-leaved and mixed varieties) occupy 32% (30% of Elbe River basin) of the area and pastures cover 12% (14% of Elbe River basin). Urbanised and other artificial surfaces except non-agricultural vegetated areas demand 7% (8% of Elbe River basin) of the area. Other land cover classes are only locally relevant, e.g. lakes.

The European Common Agricultural Policy (CAP) directly affects cropping schemes in the study region rendering it particularly interesting to investigate crop rotation impacts on the limited water resources. To solve fundamental environmental problems of water overuse and land degradation caused by agricultural intensification and specialisation, the post-2020 CAP underlines the role of crop rotations (European Commission, 2019). The existing obligation of crop diversification (i.e. growing more than one crop at any time per farm) will be upgraded to mandatory use of crop rotations in the post-2020 CAP.

### 2.2. Decision problem

Farmers set cropping objectives and define desired area shares to realise profitable production goals. We framed the crop rotation decision problem as the search for the best combination of potential crop sequences to reach the desired crop area shares. This framing simplifies the complex decision problem assuming that farmers have already decided how to arrange the crops in suitable sequences. Moreover, we assume that farmers behave rationally following economic profitability and agronomic criteria.

To illustrate the decision space, we introduce a simple example in which a farmer has decided to grow wheat, maize and barley, each on one third of the land. Suppose this farmer organises these crops in a three-year sequence of wheat followed by maize and then barley, to suppress soil pathogens. Also suppose that this farmer has three equally sized fields. The question is then: how to allocate the three crops across

the fields so that the desired area shares are met while adhering to the established crop sequence? If the farmer assigns each field to a distinct rotation year (i.e. a distinct crop in the sequence) to start the rotation, then each crop type would grow on the same area share, i.e. one third of the land. Over the years, the farmer would change the crops in each field following the established sequence implying a constant area share over time.

If all crop area shares are stable over time and all fields follow the same crop sequence, a given crop's area share in a crop mosaic equals the time share that same crop has for a given field over a long period. Moreover, a crop's area share is stable over time when the actual rotation year in a chosen crop sequence differs randomly between all fields.

We transferred this logic of decision making to a larger set of cultivated crops and available crop sequences from an individual farm to the regional scale and emulated it there. This allowed replication of the stochastic features of crop rotations as these land use dynamics cannot be reproduced in their entire complexity at large spatial scales.

### 2.3. Formalisation of the decision problem

To illustrate the formal emulation of crop rotation decisions at the regional scale, we extend the example introduced above to three different crop sequences and their combination (Table 1). The three crop sequences consist of individual arrangements of winter wheat, silage maize and winter barley. The first sequence involves all three crops, while the other two sequences comprise only two of the three crops each. The first crop sequence occupies 50% area share (see column  $p_1$  in Table 1) and the remaining sequences 25% each (see columns  $p_2$  and  $p_3$  in Table 1) in the spatial crop mosaic emerging at the regional scale. A crop's share in the mosaic can be calculated by multiplying this crop's

share in each of the sequences (see columns  $q_j$  in Table 1) by the corresponding sequence share (see columns  $p_j$  in Table 1) and summing the results over all three sequences. In this example, all crops have the same area share of one third in the crop mosaic.

The decision problem of combining crop sequences in order to meet the production goals (i.e. to reach the desired crop shares in the crop mosaic) under the conditions described above can be formally described as follows:

$$\sum_{j=1}^m p_j(CS_j|CM) \times q_{ij}(C_i|CS_j) = s_i(C_i|CM) \quad (1)$$

$$b_{j,L} \leq p_j \leq b_{j,U}$$

where  $CS_j$  = Crop sequence,  $CM$  = Crop mosaic,  $C_i$  = Crop,  $p_j$  = Share of crop sequence  $CS_j$  in crop mosaic  $CM$ ,  $q_{ij}$  = Share of crop  $C_i$  in crop sequence  $CS_j$ ,  $s_i$  = Share of crop  $C_i$  in crop mosaic  $CM$ ,  $b_{j,L}$  and  $b_{j,U}$  = Lower and upper bounds for  $p_j$ ,  $j$  = Crop sequence index,  $m$  = Total number of crop sequences and  $i$  = Crop index.

The solution of this equation is likely imperfect as not all crops will be completely distributed in a region depending on the fit between the number of crops and fields. Hence when solving this equation, the goal is to optimally approximate a given crop share distribution.

Considering the general relation between  $CM$  and  $CS_j$  in a region (see Eq. (1)), a likely combination of crop sequences can be determined if all potential crop sequences used in the region are known. The following non-linear optimisation problem can be formulated:

$$\left( \sum_{i=1}^n \sum_{j=1}^m p_j(CS_j|CM) \times q_{ij}(C_i|CS_j) - s_i(C_i|CM) \right)^2 \rightarrow \text{Min} \quad (2)$$



**Fig. 1.** Location of the study region used for the simulation in central Europe (darker coloured area) including the Elbe River basin (red boundary). Background map based on Natural Earth ([naturalearthdata.com](http://naturalearthdata.com)).

**Table 1**

Example of a stylised combination of three crop sequences  $CS_j$  ( $j = 1, 2, 3$ ) within one crop mosaic ( $CM$ ).  $CS_j$  are based on different arrangements of three crops  $C_i$  ( $i = 1, 2, 3$ ): winter wheat (WW), silage maize (SM) and winter barley (WB). (Note:  $q_j$  = share of crop  $C_i$  in crop sequence  $CS_j$ ;  $p_j$  = share of crop sequence  $CS_j$  in crop mosaic  $CM$ ;  $s_i$  = share of crop  $C_i$  in crop mosaic  $CM$ ).

		$CS_j$												
		1		2		3								
		WW-SM-WB		WW-SM-WW		WB-SM-WB		CM						
$C_i$	$q_1$	$\times$	$p_1$	+	$q_2$	$\times$	$p_2$	+	$q_3$	$\times$	$p_3$	=	$s_i$	
$i$														
1	WW	$\frac{1}{3}$		$\frac{2}{4}$		$\frac{2}{3}$		$\frac{1}{4}$		0		$\frac{1}{4}$	=	$\frac{1}{3}$
2	SM	$\frac{1}{3}$		$\frac{2}{4}$		$\frac{1}{3}$		$\frac{1}{4}$		$\frac{1}{3}$		$\frac{1}{4}$	=	$\frac{1}{3}$
3	WB	$\frac{1}{3}$		$\frac{2}{4}$		0		$\frac{1}{4}$		$\frac{2}{3}$		$\frac{1}{4}$	=	$\frac{1}{3}$
												$\sum_{i=1}^3 s_i$	=	1

with  $p_j \in [0, 1] \forall j = 1, \dots, m$ , where  $n =$  Total number of crops.

The best solution is reached when for every crop the combination of different crop sequences leads to the given crop share in the crop mosaic. The crop sequence optimisation gives the relative percentage of a crop sequence in a region which we interpret as the probability for its occurrence. However, only in an ideal case the combination of crop sequences will perfectly match the given shares for all crops. Very often some differences remain. These differences can be decreased by revising the sequences or by adding new sequences. We published the R Code to determine the occurrence probabilities for pre-defined crop sequences to match the given crop area shares under the Open Source Initiative

approved license (Conradt, 2021).

#### 2.4. Algorithm for generating spatial crop cover and its year-to-year changes

The final solution of the crop sequence optimisation, i.e. the occurrence probabilities, was used to generate an initial crop cover based on two steps: a) the spatial allocation of crop sequences and b) the selection of a starting year. We assumed crop rotations to be randomly distributed within a given region implying that the regional crop share is representative for all subunits. In our application of eco-hydrological

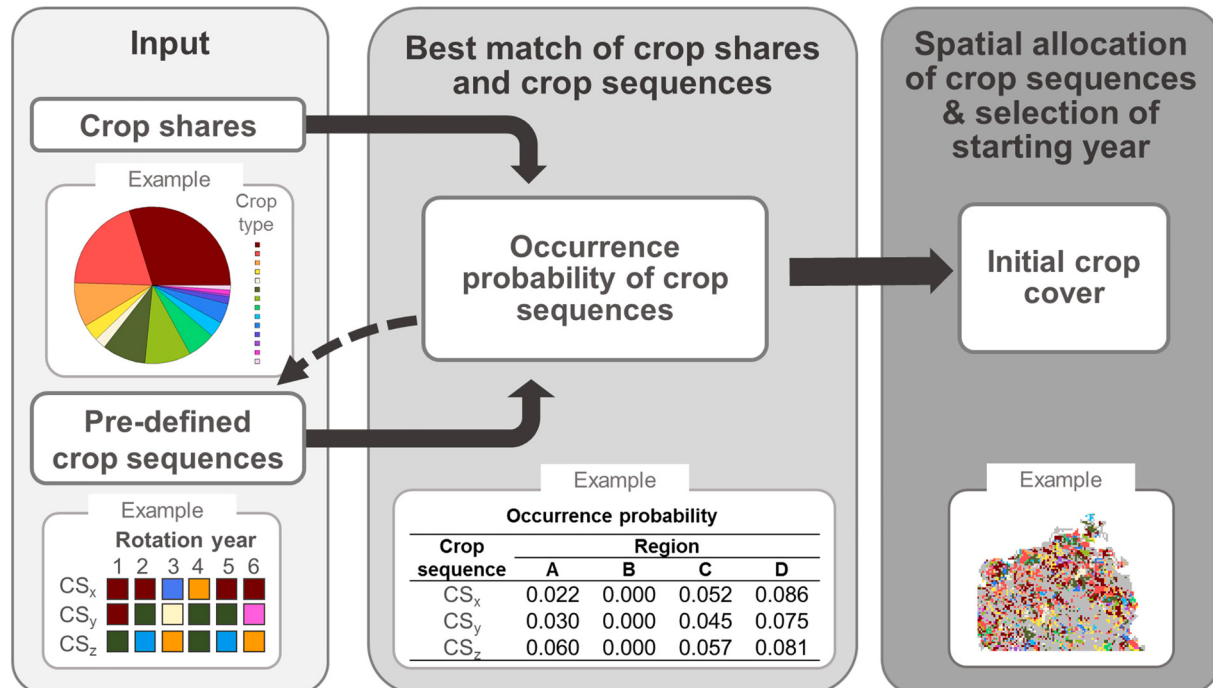


**Fig. 2.** Conceptual scheme of the Crop Generator: Emulating the decision making on crop rotations at the regional scale to replicate stochastic characteristics of crop rotations. Using the given crop share information and pre-defined crop sequences, non-linear optimisation serves to determine the occurrence probabilities for each crop sequence to match the crop area shares. Based on these occurrence probabilities, crop sequences are randomly allocated to hydrotopes (or other subunits) and an independent starting year in a sequence is chosen for each hydrotope to generate an initial crop cover (Note: CS = Crop sequence).

modelling, cropland hydrotopes are considered as subunits. Hydrotopes are characterised by homogenous land use and soil type within sub-basins and hence uniform eco-hydrological behaviour (for further details of the eco-hydrological model see [Section 2.6](#)).

Firstly, we cumulate the occurrence probabilities for all crop sequences used in a given region. This results in a [0,1] interval for each region composed of sectors whose sizes equal the occurrence probabilities of the crop sequences used in the region. The sum of all probabilities per region equals 1. In this interval, we randomly select a number indicating a specific sector in the interval. We then assign a hydrotope to the crop sequence associated with the selected number. Secondly, we randomly choose the starting year in the selected crop sequence, independent of the starting year in any other hydrotope. This procedure is repeated to determine an initial crop cover for all hydrotopes in a given region. Year-to-year crop cover dynamics follow the sequential order in the crop sequences. When a crop sequence is fully realised in a hydrotope, i.e. after finishing the final rotation year, the crop sequence starts again with the crop assigned to the first rotation year.

## 2.5. The Crop Generator

Based on the above principles, we established the Crop Generator ([Fig. 2](#)) to emulate the decision making on crop rotations at the regional scale. Using two inputs, i.e. given crop share information and pre-defined crop sequences, it serves to optimise crop sequence combinations to match the regional crop shares as good as possible and to generate an initial crop cover.

From a regional crop spectrum only those crops that have a relevant area share above a pre-defined threshold are selected. This crop spectrum can be derived from agricultural statistics or agro-economic simulations, such as the Common Agricultural Policy Regional Impact (agro-economic simulation) model CAPRI ([Britz and Witzke, 2014](#); [Blanco et al., 2017](#)), used in this study, or the regionalised agricultural and environmental information system RAUMIS ([Henrichsmeier et al., 1992](#)). Each relevant crop's share is normalised according to the sum of all crops considered in the simulation of crop rotations. Crop sequences are pre-defined considering realistic regional follow-up crops and rotation lengths. The definition of crop sequences can be informed by interviews with farmers or other experts, specialised literature and recommendations from agricultural agencies.

The combination of the pre-defined crop sequences (i.e. their occurrence probabilities) which matches best the given crop shares is determined using quadratic programming, potentially including iterative adjustments in crop sequences (see dashed arrow in [Fig. 2](#)). To solve the optimisation problem, we used the quadratic programming routine `solve.QP()` of the 'quadprog' package ([Turlach, 2019](#)) of R (version 3.5.3; [R Core Team, 2017](#)).

Using the best matching crop sequence probabilities, two random numbers are determined for each hydrotope: a) assigning a crop sequence and b) the starting year in a sequence to every relevant hydrotope.

## 2.6. Combination of Crop Generator and eco-hydrological model

To demonstrate its functionality, we combined the Crop Generator with SWIM to overcome limitations in eco-hydrological modelling related to misrepresentation of real-world cropping systems ([Hattermann et al., 2007](#)). SWIM is a spatially semi-distributed catchment model integrating hydrological processes, crop and natural vegetation growth, nutrient dynamics, stream runoff and sediment transport ([Krysanova et al., 1998](#)). SWIM was mainly developed to assess impacts of changes in land use and climate in meso- (10.000–100.000km<sup>2</sup>) to macroscale (>100.000km<sup>2</sup>) river basins. It has been extensively tested and refined in river basins worldwide and used for climate and land use impact assessments in the Elbe, Rhine, Niger, Blue Nile, Limpopo and Upper Yellow River basins ([Hattermann et al., 2005, 2007, 2011](#);

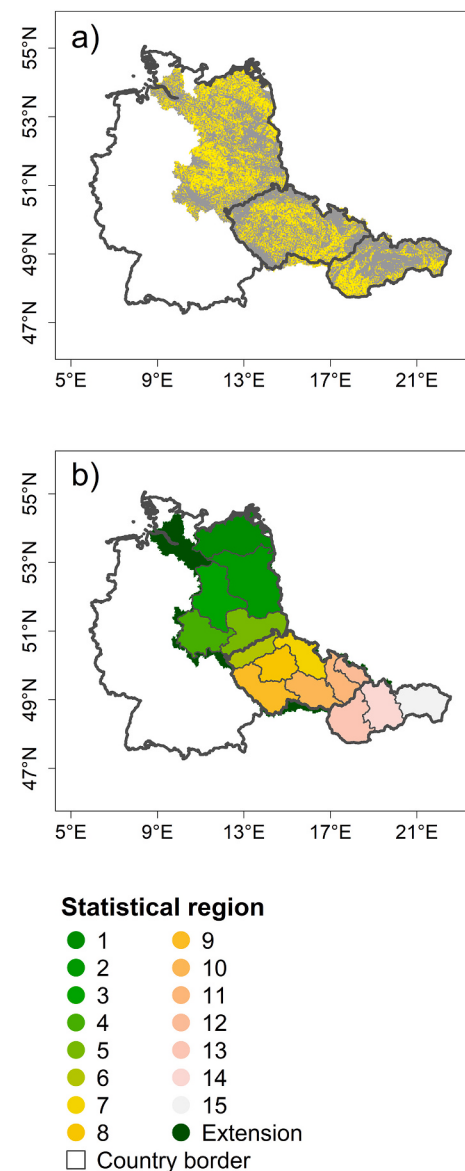


**Fig. 3.** Study region used in the simulation including a) 7,608 hydrotopes simulated with cropping activities indicated in yellow colour and b) 15 statistical regions covered by the CAPRI model.

[Krysanova et al., 2015](#)).

SWIM uses a three-level disaggregation scheme: basin – subbasins – hydrotopes. The time step in the model is daily. The vegetation module constitutes an important interface between hydrology and nutrient dynamics. It represents crops and natural vegetation. To calculate plant growth, SWIM uses plant-specific parameters defined for 76 crop/vegetation types as well as representative timings of sowing, fertilisation and harvesting included in the management routines (for detailed model description and model setup see [Krysanova et al., 1998, 2000](#); [Wortmann, 2020a, 2020b](#)).

We combined a hydrological basin and administrative areas according to the original project's specification and conducted both the hydrological and crop modelling uniformly. This allowed us to integrate a multitude of river outlets cut off by national boundaries and dry inlets in the Czech and Slovakian parts as well as splinter areas of the Elbe River basin located outside the administrative regions. This hybrid setup demonstrates how spatially incongruent and only partly overlapping data sources (i.e. river runoff and agricultural statistics) can be effectively combined for multi-criteria evaluation. The entire study region

was subdivided into 2248 subbasins and 49,641 hydrotopes. The average hydrotope size is 5.4 km<sup>2</sup> (3.7 km<sup>2</sup> in the German part of the study region and 10.4 km<sup>2</sup> in the Czech and Slovakian parts; differences owing to different national subbasin definitions and soil map inputs). SWIM simulates cropping activities in 7,608 out of the total 49,641 hydrotopes covering 40% of the entire study region (Fig. 3a).

Regional crop share information for the study region was available for 15 statistical regions at NUTS-2 level (Nomenclature of Territorial Units for Statistics; European Union, 2019) (Fig. 3b), approximated by CAPRI (Blanco, 2019; Britz and Witzke, 2014). We used CAPRI crop share estimations for the year 2010 as reference (Blanco, 2019). These estimations were not available for the entire Elbe River basin, so that we assigned the hydrotopes outside the statistical regions randomly to one of the 15 statistical regions.

We focus on 14 major crops (see Table S.1 in Supplementary Materials), each of them covering at least 0.6% of arable land in the study region. We exclude permanent, irrigated and local special crops (e.g. fruits, wine, flax, hemp, tobacco and soya). Focussing on arable land, we also disregard fodder production on pasture land. Altogether, the selected 14 crops represent 74% of the total agricultural area covered by the 15 statistical regions. This CAPRI crop share information is called ‘original’ crop share and is compared with the ‘allocated’ crop share obtained by applying the Crop Generator.

We used the 14 selected crops to pre-define 42 crop sequences based on expert suggestions and the above introduced agronomic considerations and good agricultural practices (Koennecke, 1967; Martin et al., 1976) assembling the crops in realistic six-year sequences. We fine-tuned these sequences (Table 2 and Table S.2) by iterative adjustments, e.g. increasing some crops’ share and defining additional sequences, so that the quadratic programming routine reached an acceptable solution for each of the 15 statistical regions (Table 3 and Table S.3; see also cumulated occurrence probabilities in Fig. S.1).

We parametrised the 14 crops in such a way that their management dates (i.e. sowing, fertilising, harvesting; see Table S.4) allowed a smooth follow-up of the crops assembled in the 42 crop sequences. This involved, e.g. adjusting sowing dates so that a given crop in a sequence was sown only after the preceding crop had been harvested. We used fixed parameters based on absolute days in a year (Table S.4). Using this crop parametrisation, we run the model for a 30-year period (1985–2014). Before the crop rotations actually started, we implemented summer barley sown in spring as the standard initial crop cover because each model run starts in January with fallow soils. If a winter crop was grown in the starting year in a given hydrotope, this crop was sown in autumn after the initial summer barley had been harvested.

**Table 2**

Examples of pre-defined crop sequences arranging crops in six rotation years. (For entire portfolio of 42 crop sequences see Table S.2. Abbreviations: WW = winter wheat, RA = winter rape, WB = winter barley, RY = winter rye, WC = other winter cereals, SM = silage maize, FO = other fodder on arable land, GM = grain maize, SB = summer barley, SU = sugar beet, OA = oats, AL = alfalfa, PO = potatoes, VE = other vegetables).

Crop sequence number (CS <sub>j</sub> )	Year					
	1	2	3	4	5	6
1	WW	WW	WW	WW	WW	WB
2	WW	WW	SM	WB	WW	WW
3	WW	WW	RA	WW	WW	RA
4	WW	RA	WW	RA	SM	WW
5	WW	SU	WW	SM	WW	SU
6	WB	RA	WW	WB	RA	WW
7	RY	RA	WW	WW	RA	WW
8	GM	WW	RA	GM	GM	GM
9	SM	SM	SM	SM	WW	SM
10	WW	SM	WC	SM	SM	PO

## 2.7. Validation approach

To validate the crop representation obtained from the Crop Generator, we assessed the match between the original and allocated crop shares. Firstly, we calculated deviations per crop type and statistical region. Secondly, to assess the strength of associations between the original and allocated crop shares, we calculated Pearson correlation coefficients for all crop types grown per statistical region and per crop type across all regions. Thirdly, we tested data distributions using Shapiro-Wilk normality test (Shapiro and Wilk, 1965). For non-normally distributed data, Spearman’s  $\rho$  and its extension Kendall’s  $\tau$  provide alternative measures based on data ranks. We compared the Pearson correlation coefficients with Spearman and Kendall rank correlation coefficients based on absolute cropping areas and area shares. Fourthly to discern possible area size effects, we compared crop type specific correlations with the mean hydrotope size and mean cropping area per statistical region.

## 2.8. Test of hydrological sensitivity

We assessed the sensitivity of SWIM outputs to crop rotations considering the entire study region for the 30-year period (1985–2014). We focussed on daily river discharge, runoff (surface and subsurface), groundwater seepage and evapotranspiration. We compared the water balance components simulated under crop rotations with a) a simplified winter and summer crop representation, b) winter wheat as monoculture and c) silage maize as monoculture. We run three individual simulation variants. One variant included crop rotations using the Crop Generator. The other two variants simulated either winter wheat or silage maize, the principal winter and summer crops, as a monoculture.

We used the two monoculture variants to represent the combined impacts of winter and summer crops in a simplified way. We averaged the annual area shares of all winter and summer crops grown in the crop rotations over the entire study region. We used the resulting mean shares of winter and summer crops to calculate the area-weighted average of the water balance components resulting from the separate simulations of winter wheat and silage maize. We also compared the simulated water balance components under crop rotations with the two separately simulated monocultural crops to provide a bridge to standard SWIM simulations (Krysanova et al., 2015; Hesse and Krysanova, 2016).

## 3. Results

### 3.1. Validation of crop representation

#### 3.1.1. Representation of regional crop mosaics

The mean original and allocated crop shares matched well (Fig. 4a and b) with very small mean relative deviations ranging between -1 to +2% of area share for the entire study region (Fig. 4c). Relative deviations were smallest for major winter crops (e.g. winter rape, winter rye) and common summer crops (e.g. silage maize and summer barley). The largest deviations were found for sugar beet and grain maize with small absolute cropping areas. The generally small deviations were also reflected in a high Pearson correlation between the original and allocated crop shares ( $r = 0.98$ ) for the whole study region. Yet, correlations varied across the statistical regions (Fig. 5a). Crop shares correlated best in Region 4 (Thuringia in Germany, ca. 714,000 ha of arable land and 581 hydrotopes simulated with cropping activities) and diverged most in Region 12 (Moravskoslezko in Czech Republic with only ca. 147,000 ha of arable land and 91 hydrotopes simulated with cropping activities) (Fig. 5a). Regions with smaller hydrotopes, especially Regions 1–5 located in Germany, tend to be better represented (see the higher correlation coefficients in Fig. S.2).

#### 3.1.2. Representation of crop types

The average correlation between the original and allocated crop

**Table 3**

Occurrence probabilities of ten crop sequences in selected statistical regions determined by quadratic programming. (For occurrence probabilities of all crop sequences in all 15 statistical regions see Table S.3).

Crop sequence number ( <i>CSj</i> )	Occurrence probability							
	Region 1	Region 2	Region 3	Region 4	Region 5	Region 6	Region 7	Region 8
1	0.022	0.000	0.052	0.086	0.029	0.138	0.017	0.056
2	0.030	0.000	0.045	0.075	0.032	0.076	0.020	0.039
3	0.060	0.000	0.057	0.081	0.041	0.118	0.046	0.070
4	0.067	0.000	0.049	0.069	0.045	0.056	0.049	0.052
5	0.064	0.004	0.092	0.019	0.027	0.026	0.081	0.070
6	0.062	0.002	0.038	0.079	0.063	0.065	0.048	0.060
7	0.058	0.000	0.055	0.047	0.039	0.066	0.026	0.040
8	0.000	0.000	0.000	0.000	0.000	0.000	0.007	0.000
9	0.058	0.077	0.024	0.029	0.035	0.000	0.031	0.000
10	0.008	0.000	0.010	0.018	0.025	0.000	0.000	0.000

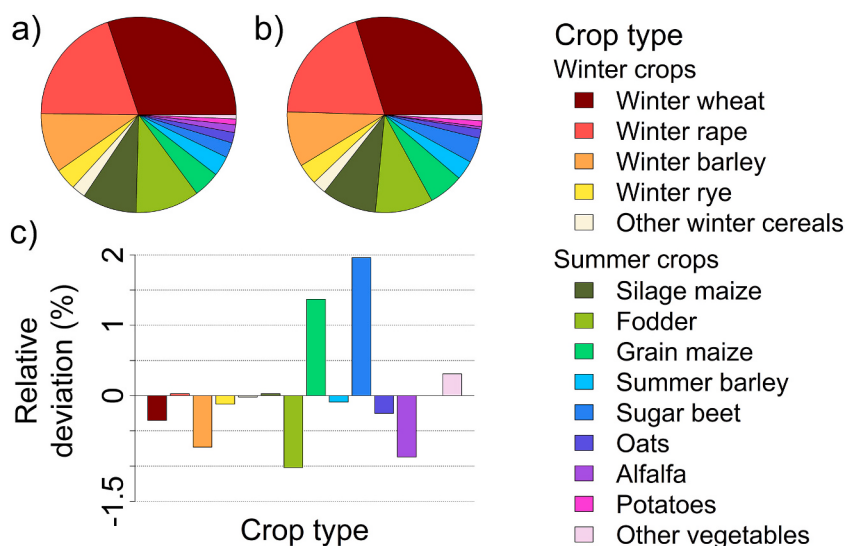


**Fig. 4.** Crop distributions for the entire study region: a) original crop shares based on CAPRI model, b) allocated crop shares obtained by applying the Crop Generator and c) relative deviations between the original and allocated crop shares.

shares across all statistical regions was high ( $r = 0.89$ ). Correlations were also very high for most winter crops and some summer crops (Fig. 5b). Crops with lower correlations were those grown only in a small area, e.g. oats, alfalfa and potatoes (see Fig. S.4).

The Shapiro–Wilk normality test (Fig. S.5) showed normal distributions of cropping areas for major winter crops (winter wheat, winter rape and winter barley) and some of the summer crops (fodder, sugar beet and alfalfa). Average correlation values were comparable between Pearson and Spearman rank correlation coefficients (Table S.5). Kendall's  $\tau$  was still relatively high ( $\tau > 0.7$ ) on average, for all winter and for the most important non-normally distributed summer crops considering absolute cropping areas across all statistical regions (see Table S.5).

### 3.2. Hydrological sensitivity to crop rotations

The test of hydrological sensitivity (see Section 2.8) was conducted for Neu Darchau, the most downstream discharge gauge of the Elbe River which integrates a basin area of 131,950 km<sup>2</sup>. The model had not been explicitly calibrated to the Neu Darchau hydrograph and we accepted runoff underestimations between 4–20% as we were interested in providing a proof-of-concept depicting the shifts of major water balance components caused by crop rotations. The comparison with the simplified winter and summer crop representation is based on 65% winter and 35% summer crop area shares representing the simulated crop rotations (see Fig. S.3 for examples of resulting crop cover

dynamics).

On average, simulations including crop rotations resulted in 5–9% higher daily river discharge compared with the simplified winter and summer crop representation and the monocultures of winter wheat and silage maize (see Table S.6 for details at five major gauges along the Elbe River). Extremes in daily discharge increased accordingly. Low flow (lowermost 15 percentiles) increased by 7–12%, whereas high flow (uppermost 15 percentiles) increased by 3–5% compared with the simplified cropping pattern representation (see Table S.7). Fig. 6 shows observed and simulated discharge extremes at Neu Darchau. The systematic under-estimation resulting from the simplified representation of cropping patterns are minimised by crop rotations, especially under low flow conditions (see also Figs. S.6–S.14 for details at five major gauges along the Elbe River).

Moreover, crop rotations resulted in higher annual runoff (12–13%) and groundwater seepage (12–16%) and lower evapotranspiration (−5 to −7%) compared with the simplified cropping pattern representation (see Table S.8). Differences in these water balance components showed clear seasonal patterns, reaching the largest values during the main growing season. In particular, runoff increased most during July and August, although in May and June silage maize monocultures resulted in higher runoff (Fig. 7a). Groundwater seepage increased most during July–September, but was again surpassed by silage maize in May and June (Fig. 7b). Evapotranspiration decreased most during June, but was surpassed by winter wheat in May and June and by silage maize in June–August (Fig. 7c).

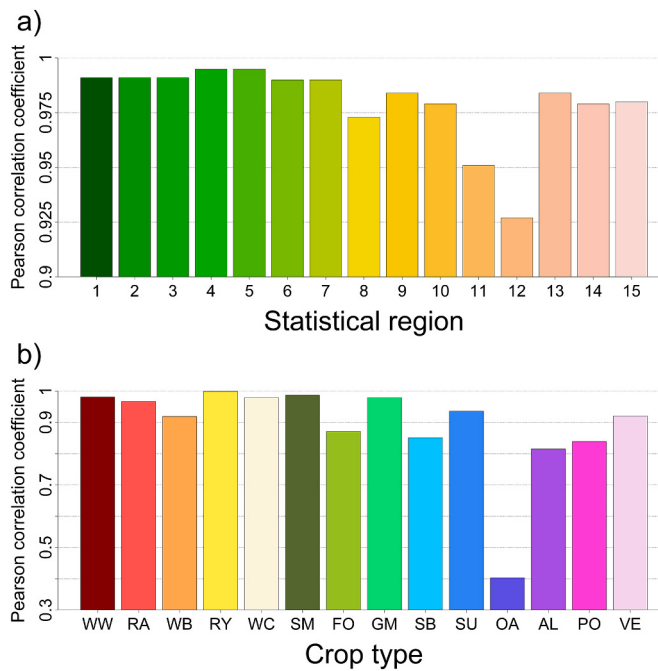


**Fig. 5.** Pearson correlation coefficients between the original and allocated crop shares a) for all crop types grown per region and b) per crop type across all regions; note the different ranges of the y-axes. (For abbreviations see Table 2).

#### 4. Discussion

The Crop Generator closes the gap between aggregated agricultural statistics and the necessity of realistically representing crop rotations in eco-hydrological modelling. It takes a two-step approach to replicate the decisions underlying the organisation of crop rotations. At first, an optimal share of the crops to be cultivated is determined and then disaggregated spatially and temporally based on the given area proportions. If the crop distribution is inappropriate, i.e. the optimisation algorithm yields no solution, the disaggregation is iteratively fine-tuned. In these iterations, new crop sequences are included to reduce the discrepancy between the original and allocated crop shares. Ideally, the aggregated crop shares of the newly defined crop sequences should be close to the shares of the misrepresented crops. Even using only a few iterations we achieved a good agreement between the original crop shares and the allocated ones obtained by applying the Crop Generator.

The overall high correlations between the original and allocated crop shares sufficiently capture the large-scale variations in crop distribution while keeping the optimisation effort at reasonable level.

The allocation of crops can be fine-tuned further to increase correlations with the original crop shares for some crops. In the optimisation process, residuals of quadratic programming provide insights in the area share per crop that could not be distributed in a given region. These residuals can be related to the original area share per crop and statistical region to indicate the remaining error. For the crops with an intolerably high error, the portfolio of crop sequences would need to be adjusted by defining additional crop sequences. A finer subdivision of the study region into smaller hydrotopes presents another way for more precisely approximating the original crop shares. When the crop sequences and the selected starting crops are assigned to large hydrotopes, they may take up disproportionate area shares exceeding the original values. The greater flexibility provided by the use of smaller hydrotopes is associated with a linearly increasing computational demand.

These refinements would need to be performed for each statistical region individually usually involving several iterations in order to find an optimal match between original and allocated crop shares. Moreover, newly defined crop sequences would need to be implemented in the eco-hydrological model which requires parameterising management dates so that harvesting and sowing dates for specific crop follow-ups are compatible.

The specifications for the Crop Generator were taken from an agro-economic model simulation to reproduce the current agricultural land use in the study region. The use of modelled data highlights the operational interface the Crop Generator provides between agro-economic and eco-hydrological modelling. This is a major step forward as the lack of time series of observational crop data at high spatial resolution (Rounsevell et al., 2003; Srinivasan et al., 2010; Schönhart et al., 2011) has so far severely limited the implementation of crop rotations in eco-hydrological models. Among the few hydrological model applications that implemented crop rotations, remote sensing based land cover maps served to construct short crop sequences assigned to hydrological response units (Srinivasan et al., 2010; Parajuli et al., 2013; Gao et al., 2017). This was sometimes done in an automated way with management operations updated accordingly (Rivas-Tabares et al., 2019). Considering a finer temporal resolution, dominant seasonal land use trajectories were also manually implemented for one year (Nkwasa et al., 2020). However, translating multi-year crop cover data into crop rotations entails not only high costs and considerable efforts (Leenhardt et al., 2010) due to the need to correct frequently occurring classification errors (Mueller-Warrant et al., 2016). It also involves potential

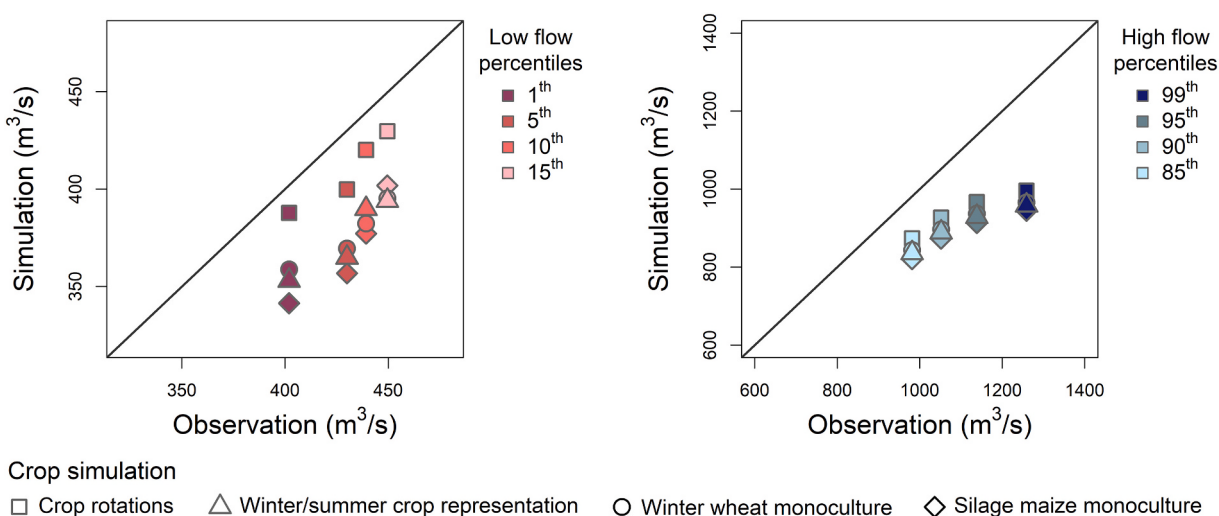


**Fig. 6.** Comparison of observed and simulated extremes in long-term mean daily discharge (1985–2014) at Neu Darchau assuming different crop representations.

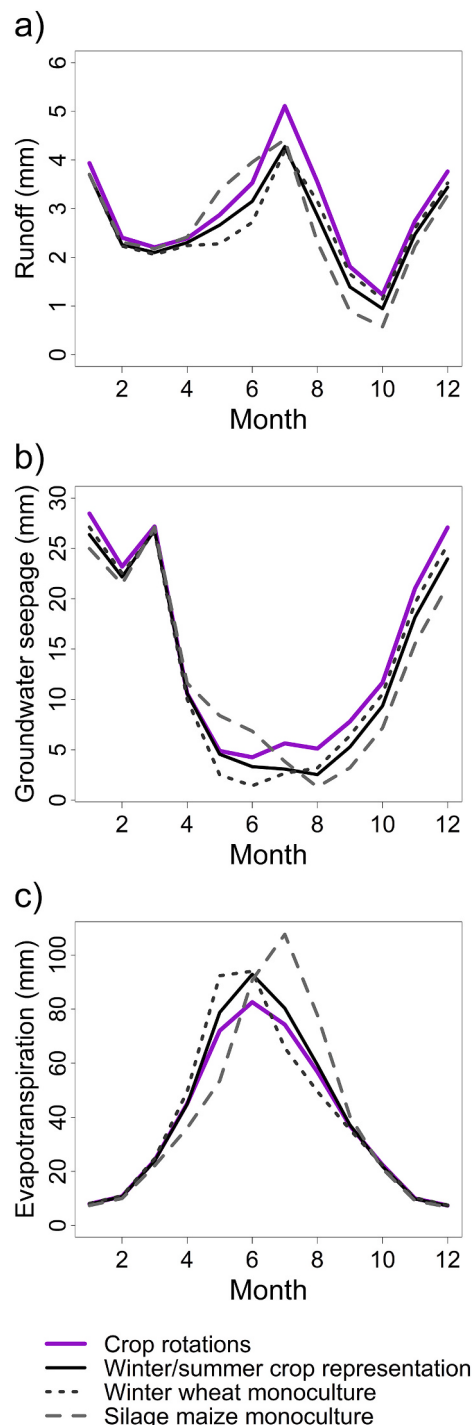


**Fig. 7.** Comparison of long-term monthly means in hydrological components (1985–2014) simulated in agricultural hydrotopes based on crop rotations, the simplified winter and summer crop representation and the monocultures of winter wheat and silage maize. Here: a) runoff (surface and subsurface), b) groundwater seepage and c) evapotranspiration.

legislative and tax-related issues indicating data sensitivity (e.g. access to Land Parcel Identification System data is restricted to protect privacy and scientific data analyses require special permission). The Crop Generator provides a more effective way to implement crop rotations, particularly in large scale eco-hydrological modelling. With the operational interface, the Crop Generator can also be used to translate possible future effects of modifications in policy frameworks and agricultural markets into crop share and land use changes.

The hydrological sensitivity test confirmed that the eco-hydrological model responds to the implementation of crop rotations. The increases in daily river discharge, runoff and groundwater seepage are consistent with the decreases in evapotranspiration underlining the role of vegetation in splitting the precipitation flux. The change in discharge could be explained by the dense foliage (i.e. high leaf area index) of silage maize and the earlier development of young winter wheat plants inducing higher interception losses and higher evapotranspiration. This contributes to lower discharge levels than those found in crop rotations. Overall, the crop rotation effects shown in this paper imply better water availability for crops particularly during extremely dry conditions. This demonstrates that the emulation of crop rotation decisions is relevant for eco-hydrological impact assessments. The differences specified in Section 3.2 indicate the typical error range resulting from the simplistic representation of cropping patterns. Individual simulations of all crops as monocultures and the subsequent area-weighted averaging of results would provide further details on how far the simplified representation of cropping patterns may converge with the use of crop rotations.

Explicit implementation of crop rotations also improved the simulation of agricultural impacts on water balance components in other studies. For example, discharge, soil moisture and evapotranspiration were more accurately simulated by a hydrological model that was coupled with a crop model considering crop rotations (Zhang et al., 2021). This demonstrates potential for improving crop growth models that currently simulate hydrological processes in a simplified way (De Wit et al., 2019) in order to more precisely evaluate restoration, climate adaptation and sustainable intensification strategies (Amjath-Babu et al., 2016; Sietz et al., 2017; Cholo et al., 2019; Vidal Merino et al., 2019; Shukla et al., 2021). However less sophisticated than our approach, Zhang et al. (2021) considered only four major crops in two-year sequences. Yang et al. (2020) and Dakhllalla et al. (2016) implemented and tested the effects of specific crop sequences separately, impeding a clear understanding of combined hydrological effects at regional scale. The lack of accounting for spatially varying crop sequence frequencies highlights the advances of the more complex, spatially-differentiated approach presented in this paper. Emerging large-scale spatial data on land use and programming interfaces (Gorelick et al., 2017; Zhang et al., 2020) provide promising opportunities for systematically implementing crop rotations at high spatial and temporal resolution.

The current version of the Crop Generator distributes the crop types randomly across the subunits, i.e. hydrotopes, within statistical regions. As an extension, crop rotations can be distributed along gradients using an indicator variable (e.g. soil fertility or potential wheat yield) to approximate the crop distribution even more realistically in future applications. In this gradient-dependent distribution, the spatial subunits would be classified according to a selected indicator. For each class, the original crop shares would be aggregated and then translated into combinations of relevant crop sequences. Hence, crop sequences are not allocated within the statistical regions, but within the newly determined gradient classes.

We used fixed cropping schemes assuming that deviations from determined management dates will statistically average out over time. This aimed at balancing the programming and computational efforts with the large extent and detailed spatial discretisation of the study region. In reality though, unexpected weather conditions, e.g. delayed rainfall or cold seasons, may delay the maturing of crops. As farmers have a certain flexibility to adjust crop management to this variability, relative management dates may be parametrised in future applications, e.g. based on accumulated temperature sums.

## 5. Conclusions

We presented the Crop Generator as a solution to simulate more realistic cropping patterns in large-scale eco-hydrological modelling. The Crop Generator emulates farmers' decision making at the regional

scale enabling an efficient implementation of crop rotations and plausible reproduction of cropping patterns. By combining it with an eco-hydrological model, we demonstrated the sensitivity of key hydrological processes to crop rotations in a central European region. The Crop Generator methodology can be transferred to other regions where comparable input data – regional cropping area or crop share statistics and typical or exemplary crop sequences – are available and crop rotations are relevant.

The more realistic representation of crop rotations extends the range of problems that can be studied with higher accuracy using eco-hydrological modelling. Environmental consequences of agricultural policy changes, such as those resulting from the mandatory application of crop rotations required by the post-2020 CAP (European Commission, 2019), can now be explored more accurately. Beside the demonstrated hydrological effects on river discharge, runoff, groundwater seepage and evapotranspiration, future applications may further explore likely effects on soil water, crop yield patterns, nutrient cycles and erosion.

The good replication of regional crop shares not only allows to simulate current but also future conditions, after an adjustment of management dates and use of flexible dates. In particular, the Crop Generator enables projections of future changes in crop rotations in view of climate and socio-economic changes fostering more realistic scenario impact assessments. An extension of the Crop Generator to spatially distribute crop sequences according to soil types would contribute to further fine-tuning the realism of eco-hydrological modelling.

## Author contributions

D.S., F.H. and F.W. designed the research; FW contributed and formalised the Crop Generator concept, D.S. and T.C. performed the research; D.S. analysed the data and wrote the paper. T.C., V.K., F.H. and F.W. contributed to the discussion of results and the writing of the paper. We kindly thank Michael Wortmann for his swift programming support. This study contributes to the Global Land Programme <https://glp.earth>.

## Funding

This work was supported by the Horizon 2020 project SIM4NEXUS [grant no. 689150] and the Horizon 2020 project Oasis Innovation Hub for Catastrophe and Climate Extremes Risk Assessment (grant no. 730381).

## Declaration of Competing Interest

The authors declare that they have no known competing financial interests or personal relationships that could have appeared to influence the work reported in this paper.

## Appendix A. Supplementary Materials

Supplementary Materials to this article can be found online at <https://doi.org/10.1016/j.agryea.2021.103183>.

## References

- Amjath-Babu, T.S., Krupnik, T.J., Kaechele, H., Aravindakshan, S., Sietz, D., 2016. Transitioning to groundwater irrigated intensified agriculture in Sub-Saharan Africa: an indicator based assessment. *Agric. Water Manag.* 168, 125–135. <https://doi.org/10.1016/j.agwat.2016.01.016>.
- Bainard, L.D., Navarro-Borrell, A., Hamel, C., Braun, K., Hanson, K., Gan, Y., 2017. Increasing the frequency of pulses in crop rotations reduces soil fungal diversity and increases the proportion of fungal pathogens in a semiarid agroecosystem. *Agric. Ecosyst. Environ.* 240, 206–214.
- Barbieri, P., Pellerin, S., Nesme, T., 2017. Comparing crop rotations between organic and conventional farming. *Sci. Rep.* 7 (1), 13761. <https://doi.org/10.1038/s41598-017-14271-6>.
- Bauwe, A., Kahle, P., Lennartz, B., 2019. Evaluating the SWAT model to predict streamflow, nitrate loadings and crop yields in a small agricultural catchment. *Adv. Geosci.* 48, 1–9. <https://doi.org/10.5194/adgeo-48-1-2019>.
- Blanco, M., 2019. CAPRI-Water baseline results 2010–2050. CAPRI-Water simulations in the framework of SIM4NEXUS (Sustainable Integrated Management FOR the NEXUS of water-land-food-energy-climate for a resource-efficient Europe) project. In: EU H2020, No. 689150.
- Blanco, M., Ramos, F., Van Doorslaer, B., Martínez, P., Fumagalli, D., Ceglar, A., Fernández, F.J., 2017. Climate change impacts on EU agriculture: a regionalized perspective taking into account market-driven adjustments. *Agric. Syst.* 156, 52–66.
- Britz, W., Witzke, P., 2014. CAPRI Model Documentation, p. 2014. Available at: [http://www.capri-model.org/docs/capri\\_documentation.pdf](http://www.capri-model.org/docs/capri_documentation.pdf).
- Cholo, T., Fleskens, L., Sietz, D., Peerlings, J., 2019. Land fragmentation, climate adaptation and food security in the Gamo Highlands of Ethiopia. *Agric. Econ.* 50 (1), 39–49. <https://doi.org/10.1111/agec.12464>.
- CLC, 2012. Corine Land Cover. Version 2020.20u1. Available at: <http://land.copernicus.eu/pan-european/corine-land-cover/clc-2012>.
- Conradt, T., 2021. Crop Generator R Code. Zenodo. <https://doi.org/10.5281/zenodo.4704561>. Published on 20 April 2021.
- Dakhllalla, O.A., Parajuli, P.B., Ouyang, Y., Schmitz, D.W., 2016. Evaluating the impacts of crop rotations on groundwater storage and recharge in an agricultural watershed. *Agric. Water Manag.* 163, 332–343. <https://doi.org/10.1016/j.agwat.2015.10.001>.
- Dalin, C., Wada, Y., Kastner, T., Puma, M.J., 2017. Groundwater depletion embedded in international food trade. *Nature* 543, 700–704. <https://doi.org/10.1038/nature21403>.
- De Wit, A., Boogaard, H., Fumagalli, D., Janssen, S., Knapen, R., van Kraalingen, D., Sutip, van der Wijngaart, R., van Diepen, K., 2019. 25 years of the WOFOST cropping systems model. *Agric. Syst.* 168, 154–167.
- Dogliotti, S., Rossing, W.A.H., Van Ittersum, M.K., 2004. Systematic design and evaluation of crop rotations enhancing soil conservation, soil fertility and farm income: a case study for vegetable farms in South Uruguay. *Agric. Syst.* 80 (3), 277–302. <https://doi.org/10.1016/j.agryea.2003.08.001>.
- Dudley, N., Alexander, S., 2017. Agriculture and biodiversity: a review. *Biodiv* 18 (2–3), 45–49. <https://doi.org/10.1080/14888386.2017.1351892>.
- Dury, J., Schaller, N., Garcia, F., Reynaud, A., Bergez, J.E., 2012. Models to support cropping plan and crop rotation decisions. A review. *Agron. Sustain. Dev.* 32 (2), 567–580. <https://doi.org/10.1007/s13593-011-0037-x>.
- Epelde, A.M., Cerro, I., Sánchez-Pérez, J.M., Sauvage, S., Srinivasan, R., Antiguedad, I., 2015. Application of the SWAT model to assess the impact of changes in agricultural management practices on water quality. *Hydrol. Sci. J.* 60 (5), 825–843. <https://doi.org/10.1080/02626667.2014.967692>.
- European Commission, 2019. The Post-2020 Common Agricultural Policy: Environmental Benefits and Simplification. Directorate-General for Agriculture and Rural Development, Bruxelles, Belgium.
- European Union, 2019. Methodological Manual on Territorial Typologies — 2018 Edition. Publications Office of the European Union, Luxembourg. <https://doi.org/10.2785/930137>. Available at: <https://ec.europa.eu/eurostat/documents/3859598/89507230/KS-GQ-18-008-EN-N.pdf/a275fd66-b56b-4ace-8666-f39754ede66b>.
- Franke, A.C., Van den Brand, G.J., Vanlaue, B., Giller, K.E., 2018. Sustainable intensification through rotations with grain legumes in sub-Saharan Africa: a review. *Agric. Ecosyst. Environ.* 261, 172–185. <https://doi.org/10.1016/j.agee.2017.09.029>.
- Gao, J., Sheshukov, A.Y., Yen, H., Kastens, J.H., Peterson, D.L., 2017. Impacts of incorporating dominant crop rotation patterns as primary land use change on hydrologic model performance. *Agric. Ecosyst. Environ.* 247, 33–42.
- Gorelick, N., Hancher, M., Dixon, M., Ilyushchenko, S., Thau, D., Moore, R., 2017. Google Earth Engine: planetary-scale geospatial analysis for everyone. *Remote Sens. Environ.* 202, 18–27. <https://doi.org/10.1016/j.rse.2017.06.031>.
- Graumann, K., Rubio Dellepiane, V., Terra, J.A., Quincke, J.A., 2020. Long-term observations in contrasting crop-pasture rotations over half a century: statistical analysis of chemical soil properties and implications for soil sampling frequency. *Agric. Ecosyst. Environ.* 287 (Art. No. 106710).
- Hattermann, F.F., Wattenbach, M., Krysanova, V., Wechsung, F., 2005. Runoff simulations on the macroscale with the ecohydrological model SWIM in the Elbe catchment—validation and uncertainty analysis. *Hydrol. Proced.* 19 (3), 693–714. <https://doi.org/10.1002/hyp.5625>.
- Hattermann, F.F., Gömann, H., Conradt, T., Kaltfotef, M., Kreins, P., Wechsung, F., 2007. Impacts of global change on water-related sectors and society in a transboundary Central European river basin. Part 1: project framework and impacts on agriculture. *Adv. Geosci.* 11, 85–92. <https://doi.org/10.5194/adegeo-11-85-2007>.
- Hattermann, F.F., Weiland, M., Huang, S., Krysanova, V., Kundzewicz, Z.W., 2011. Model-supported impact assessment for the water sector in central Germany under climate change - a case study. *Water Resour. Manag.* 25 (13), 3113–3134. <https://doi.org/10.1007/s11269-011-9848-4>.
- Henrichsmeier, W., Dehio, J., Van Kampen, R., Kreins, P., Strotmann, B., 1992. Aufbau eines computergestützten regionalisierten Agrar- und Umweltinformationssystems für die Bundesrepublik Deutschland, Endbericht (Modellbeschreibung). Bonn, Germany.
- Hesse, C., Krysanova, V., 2016. Modelling climate and management change impacts on water quality and in-stream processes in the Elbe River basin. *Water* 8 (2), 40. <https://doi.org/10.3390/w8020040>.
- Koencke, G., 1967. Fruchtfolgen. VEB Deutscher Landwirtschaftsverlag, Berlin, Germany.
- Krysanova, V., Müller-Wohlfeil, D.-I., Becker, A., 1998. Development and test of a spatially distributed hydrological/water quality model for mesoscale watersheds. *Ecol. Model.* 106 (2–3), 261–289. [https://doi.org/10.1016/S0304-3800\(97\)00204-4](https://doi.org/10.1016/S0304-3800(97)00204-4).
- Krysanova, V., Wechsung, F., Arnold, J., Srinivasan, R., Williams, J., 2000. SWIM - Soil and Water Integrated Model. User Manual. PIK Report 69, Potsdam Institute for

- Climate Impact Research, Potsdam, Germany. Available at: <https://www.pik-potsdam.de/research/publications/pikreports/files/pr69.pdf>.
- Krysanova, V., Hattermann, F.F., Huang, S., Hesse, C., Vetter, T., Liersch, S., Koch, H., Kundzewicz, Z.W., 2015. Modelling climate and land-use change impacts with SWIM: lessons learnt from multiple applications. *Hydrol. Sci. J.* 60 (4), 606–635. <https://doi.org/10.1080/02626667.2014.925560>.
- Lawes, J.B., Gilbert, J.H., 1894. Rotation of crops. *J. R. Agric. Soc. Engl.* 5, 585–646 (ISSN 0080-4134).
- Leenhardt, D., Angevin, F., Biarnès, A., Colbach, N., Mignolet, G., 2010. Describing and locating cropping systems on a regional scale. A review. *Agron. Sustain. Dev.* 30, 131–138.
- Martin, J.H., Leonard, W.H., Stamp, D.L., 1976. Principles of Field Crop Production, 3rd edition. Macmillan Publishing Co., Inc., New York, NY.
- Maxime, F., Mollet, J.M., Papy, F., 1995. Aide au raisonnement de l'assoulement en grande culture. *Cah Agric.* 4, 351–362.
- Montgomery, D.R., 2007. Soil erosion and agricultural sustainability. *Proc. Nat. Acad. Sci.* 104 (33), 13268–13272. <https://doi.org/10.1073/pnas.0611508104>.
- Mueller-Warrant, G.W., Sullivan, C., Anderson, N., Whittaker, G.W., 2016. Detecting and correcting logically inconsistent crop rotations and other land-use sequences. *Internat J. Rem. Sens.* 37 (sup1), 29–59. <https://doi.org/10.1080/01431161.2016.1184354>.
- Nkwasa, A., Chawanda, C.J., Msigwa, A., Komakech, H.C., Verbeiren, B., van Griensven, A., 2020. How Can We Represent Seasonal Land Use Dynamics in SWAT and SWAT+ Models for African Cultivated Catchments? *Water* 12 (6), 1541. <https://doi.org/10.3390/w12061541>.
- Parajuli, P.B., Jayakody, P., Sassenrath, G.F., Ouyang, Y., Pote, J.W., 2013. Assessing the impacts of crop-rotation and tillage on crop yields and sediment yield using a modeling approach. *Agric. Water Manag.* 119, 32–42.
- Peng, H., Jia, Y., Tague, C., Slaughter, P., 2015. An eco-hydrological model-based assessment of the impacts of soil and water conservation management in the Jinghe River Basin, China. *Water* 7, 6301–6320. <https://doi.org/10.3390/w7116301>.
- Pérez-Gutiérrez, J.D., Kumar, S., 2019. Simulating the influence of integrated crop-livestock systems on water yield at watershed scale. *J. Environ. Manag.* 239, 385–394. <https://doi.org/10.1016/j.jenvman.2019.03.068>.
- R Core Team, 2017. R: A Language and Environment for Statistical Computing. R Foundation for Statistical Computing, Vienna, Austria. URL <https://www.R-project.org/>.
- Rivas-Tabares, D., Tarquis, A.M., Willaarts, B., De Miguel, A., 2019. An accurate evaluation of water availability in sub-arid Mediterranean watersheds through SWAT: Cega-Eresma-Adaja. *Agric. Water Manag.* 212, 211–225. <https://doi.org/10.1016/j.agwat.2018.09.012>.
- Rounsevell, M.D.A., Annett, J.E., Audsley, E., Mayr, T., Reginster, I., 2003. Modelling the spatial distribution of agricultural land use at the regional scale. *Agric. Ecosyst. Environ.* 95 (2–3), 465–479.
- Schönhart, M., Schmid, E., Schneider, U.A., 2011. CropRota – a crop rotation model to support integrated land use assessments. *Eur. J. Agron.* 34 (4), 263–277. <https://doi.org/10.1016/j.eja.2011.02.004>.
- Sedlmayr, E., 1927. Fruchfolgen und die Aufstellung des Fruchtfolgeplanes: Ein Beitrag zur Organisation des Feldbetriebes. Verlagsbuchhandlung Paul Parey, Berlin, Germany.
- Shapiro, S.S., Wilk, M.B., 1965. An analysis of variance test for normality (complete samples). *Biometrika* 52 (3/4), 591–611. <https://doi.org/10.2307/2333709>.
- Shukla, R., Gleixner, S., Yalew, A., Schauberger, B., Sietz, D., Gornott, C., 2021. Dynamic vulnerability of smallholder agricultural systems in the face of climate change for Ethiopia. *Environ. Res. Lett.* 16 (4), 044007. <https://doi.org/10.1088/1748-9326/abdb5c>.
- Sietz, D., Fleskens, L., Stringer, L.C., 2017. Learning from non-linear ecosystem dynamics is vital for achieving Land Degradation Neutrality. *Land Degrad. Dev.* 28, 2308–2314. <https://doi.org/10.1002/ldr.2732>.
- Simon, M., Bekele, V., Kulásová, B., Maul, C., Oppermann, R., Řehák, P., 2005. Die Elbe und ihr Einzugsgebiet – Ein geographisch-hydrologischer und wasserwirtschaftlicher Überblick. Internationale Kommission zum Schutz der Elbe, Magdeburg, 258 pp. URL [https://www.ikse-mkol.org/fileadmin/media/user\\_upload/D/06\\_Publikationen/07\\_Verschiedenes/2005\\_IKSE-Elbe-und-ihr-Einzugsgebiet.pdf](https://www.ikse-mkol.org/fileadmin/media/user_upload/D/06_Publikationen/07_Verschiedenes/2005_IKSE-Elbe-und-ihr-Einzugsgebiet.pdf). last accessed in April 2021.
- Srinivasan, R., Zhang, X., Arnold, J., 2010. SWAT ungauged: hydrological budget and crop yield predictions in the upper Mississippi River basin. *Transact. ASABE* 53 (5), 1533–1546. <https://doi.org/10.13031/2013.34903>.
- Turlach, B.A., 2019. Functions to Solve Quadratic Programming Problems. Package ‘quadprog’. Version 1.5-8. Available at: <https://cran.r-project.org/web/packages/quadprog/quadprog.pdf>.
- Vidal Merino, M., Sietz, D., Jost, F., Berger, U., 2019. Archetypes of climate vulnerability: a mixed-method approach applied in the Peruvian Andes. *Clim. Dev.* 11 (5), 418–434. <https://doi.org/10.1080/17565529.2018.1442804>.
- Wortmann, M., 2020a. The m.swim.\* Modules. Available at: <http://www.pik-potsdam.de/~wortmann/m.swim/>. Last access 20 November 2020.
- Wortmann, M., 2020b. The GRASS7 Soil and Water Integrated Model (SWIM) Pre-processor. Available at: <https://github.com/mwort/m.swim>; Last access 20 November 2020.
- Yang, X., Zhou, L., Song, C., Quan, C., Jianqiang, D., Xingfa, L., Yuying, S., 2020. Cropping system productivity and evapotranspiration in the semiarid Loess Plateau of China under future temperature and precipitation changes: an APSIM-based analysis of rotational vs. continuous systems. *Agric. Water Manag.* 229, 105959. <https://doi.org/10.1016/j.agwat.2019.105959>.
- Zhang, C., Di, L., Yang, Z., Lin, L., Hao, P., 2020. AgKit4EE: a toolkit for agricultural land use modeling of the conterminous United States based on Google Earth Engine. *Environ. Model. Softw.* 129, 104694. <https://doi.org/10.1016/j.envsoft.2020.104694>.
- Zhang, Y., Wu, Z., Singh, V.P., He, H., He, J., Yin, H., Zhang, Y., 2021. Coupled hydrology-crop growth model incorporating an improved evapotranspiration module. *Agric. Water Manag.* 246, 106691. <https://doi.org/10.1016/j.agwat.2020.106691>.